

Highly efficient single-photon emission from single quantum dots within a two-dimensional photonic band-gap

M. Kaniber,* A. Laucht, T. Hürlimann, M. Bichler, R. Meyer, M.-C. Amann, and J. J. Finley
Walter Schottky Institut, Technische Universität München, Am Coulombwall 3, D-85748 Garching, Germany
 (Received 26 October 2007; revised manuscript received 5 December 2007; published 28 February 2008)

We report highly efficient single-photon generation from InGaAs self-assembled quantum dots emitting within a two-dimensional photonic band-gap. A strongly suppressed multiphoton probability is obtained for single quantum dots in bulk GaAs and those emitting into the photonic band-gap. In the latter case, photoluminescence saturation spectroscopy is employed to measure a ~ 16 times enhancement of the average photon extraction efficiency, when compared to quantum dots in bulk GaAs. For quantum dots in the photonic crystal, we measure directly the external quantum efficiencies up to 25%, much higher than for dots on the same sample without a tailored photonic environment. The results show that efficient quantum dot single-photon sources can be realized, without the need for complex nanopositioning techniques.

DOI: [10.1103/PhysRevB.77.073312](https://doi.org/10.1103/PhysRevB.77.073312)

PACS number(s): 73.21.La, 42.50.Ct, 42.50.Dv, 42.70.Qs

Practical and highly efficient single-photon sources are a fundamental prerequisite for elementary quantum optics, quantum cryptography,¹ and linear optical quantum computation.² Such devices should emit one and only one photon on demand at a defined frequency and with high external quantum efficiency (η). Over the last decade, single-photon sources have been demonstrated using many different approaches, such as single atoms,³ molecules,^{4,5} color centers in solids,⁶ and semiconductor quantum dots (QDs).⁷ However, most of these approaches suffer from a very low η limiting the potential advantages they offer, when compared to highly attenuated coherent pulses. The highest values of η have been achieved using QDs coupled to various kinds of optical microresonators, such as microdisks,⁸ microposts,⁹ and photonic crystal (PC) nanocavities.¹⁰ However, the coupling of single QDs to nanocavity modes is technologically very challenging, requiring precise spatial positioning of the dots and spectral tuning of their emission frequency to match the cavity mode. Here, we propose a much simpler route toward high η , QD based single-photon sources. Our approach is based on photonic band-gap (PBG) materials to realize efficient single-photon sources, without the need for the challenging nanofabrication needed for a nanocavity source. When combined with the planar geometry of two-dimensional (2D) PCs, which greatly simplifies the incorporation of electrical contacts,¹¹ such native PBG single-photon sources may be highly advantageous for applications in quantum information science and solid state quantum optics.

In this Brief Report, we present detailed optical studies of single self-assembled In_{0.5}Ga_{0.5}As QDs, both inside and outside a photonic environment created by a 2D PC nanostructure. Randomly positioned QDs inside the PC are shown to emit photons much more efficiently when compared to those in the unpatterned substrate. This effect is shown to be due to the efficient spatial redistribution of the single-photon spontaneous emission (SE) caused by the 2D-PBG.¹² Photon correlation measurements performed on QDs in bulk GaAs and in PCs both exhibit clear photon antibunching, proving the single-photon character of the emission. Power dependent photoluminescence (PL) measurements recorded with pulsed excitation reveal that photons emitted from QDs in the PC

can be collected up to ~ 16 times more efficiently than those from QDs in bulk GaAs. Furthermore, we measure maximum values of $\eta \sim 25\%$ demonstrating the great potential of single QDs in PCs as highly efficient and practical single-photon sources.

Our structure consists of an undoped GaAs substrate onto which a 500 nm thick Al_{0.8}Ga_{0.2}As sacrificial layer was deposited by molecular beam epitaxy. Following this, a 180 nm thick GaAs waveguide was grown with a single layer of self-assembled InGaAs QDs embedded at the midpoint. PC nanostructures consisting of a triangular lattice of air holes were subsequently fabricated using standard e-beam lithography and reactive ion etching. In a final process step, a freestanding GaAs membrane was established by HF wet chemical etching. Full details of the sample structure and processing techniques can be found in Ref. 13.

The sample was mounted in a liquid He-flow cryostat (15 K) and excited by 2 ps duration optical pulses delivered from a mode-locked Ti:sapphire laser at a repetition rate of $f_{\text{laser}}=80$ MHz. The excitation wavelength was chosen to be $\lambda_{\text{exc}}=850$ nm into the quasi-two-dimensional wetting layer states beneath the QDs. The emission from the sample was collected by a 100 \times microscope objective (numerical aperture=0.8) providing submicron spatial resolution and was analyzed using a 0.5 m imaging monochromator. For detection, we used a Si based charged coupled device (CCD) camera for μ -PL experiments, a single silicon avalanche photodiode (temporal resolution of ~ 350 ps) for time-resolved spectroscopy, or a pair of similar detectors in a Hanbury Brown–Twiss¹⁶ configuration for measuring the temporal statistics of the SE from single dots.¹⁷

Under weak optical excitation, the QD ensemble emits between 890 and 960 nm, as shown in Fig. 1(a). The observed properties are typical for InGaAs QDs, e.g., linear and quadratic behaviors of the intensity of single (X) and biexciton (2X) transitions on excitation power, respectively. Typical SE decay lifetimes for excitons were around 0.6 ns as found previously from ensemble measurements.¹³ To ensure that the QDs emit deep inside the PBG, we calculated the three-dimensional photonic band structure for the structures with $r/a=0.335$, where r is the radius of the air holes and

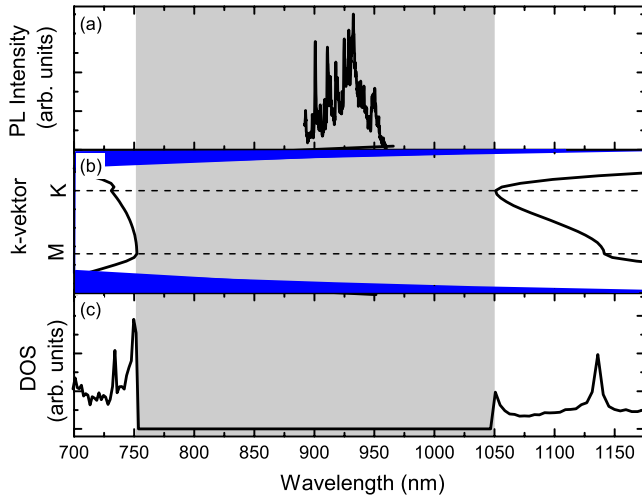


FIG. 1. (Color online) (a) μ -PL spectrum recorded from a QD ensemble. (b) Three-dimensional calculation of the photonic band structure for the GaAs 2D-PC slab with $r/a=0.335$, lattice constant $a=280$ nm, and thickness $d=180$ nm. The dark blue region denotes the light cone. (c) Calculated 3D photonic density of states for light propagation in the plane of the PC slab (only guided modes in the free space light cone) as a function of the wavelength. The gray region denotes the 2D-PBG.

$a=280$ nm the lattice constant of the PC. The simulated r/a ratio is obtained from scanning electron microscopy images of the investigated PCs. The calculated photonic band structure is presented in Fig. 1(b), showing the continuum photonic band edges (black solid lines), the appearance of a 2D-PBG (gray shaded region) for TE-like polarized light from ~ 750 to ~ 1050 nm, and the light cone (blue shaded region). The emission of the QD ensemble lies spectrally deep inside the PBG, such that the SE and spatial distribution is strongly modified.¹³ To assess the strength of these effects, we calculated the three-dimensional (3D) photonic density of states including only guided modes below the free space light cone^{14,15} experienced by a randomly positioned QD emitter in the system. These calculations clearly exhibit a strong suppression of the total photonic density of states within the spectral region of the PBG [Fig. 1(c)], as expected. The 2D-PBG results in a decreased number of optical modes in the plane of the PC into which the QDs can emit. Therefore, the QD emission is spatially redistributed and directed perpendicular to the sample surface.¹³ On the basis of these considerations, one would expect that the emission can be significantly more efficiently collected using a standard optical setup.

In Fig. 2(a), we compare pulsed μ -PL measurements recorded from a particularly bright single QD measured in bulk GaAs (labeled QD_{bulk} , $\lambda_{QD_{bulk}}=918.64$ nm), next to the PC, with a typical pair of single dots embedded randomly within the body of the PC (labeled QD_{PC1} , $\lambda_{QD_{PC1}}=923.59$ nm; QD_{PC2} , $\lambda_{QD_{PC2}}=944.80$ nm). These data were recorded using intermediate excitation power (10 W cm^{-2}) and a CCD multichannel detector. Clearly, the normalized PL intensities of QD_{PC1} and QD_{PC2} appear to be much higher than QD_{bulk} when measured under similar excitation conditions, an ob-

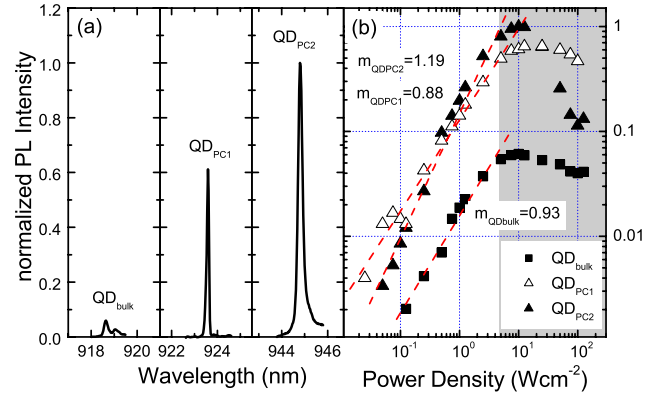


FIG. 2. (Color online) (a) μ -PL spectra of single QDs in bulk GaAs (QD_{bulk}) and in PC nanostructures (QD_{PC1} , QD_{PC2}) recorded with an excitation power of 10 W cm^{-2} . (b) Power dependent measurements for all three QDs indicating ground state emission due to the linear behavior. The gray shaded region indicates the saturation regime.

servation that already indicates that the 2D-PBG serves to spatially redistribute the SE from QD_{PC1} and QD_{PC2} , when compared to QD_{bulk} .¹⁸ In order to quantitatively test this expectation, we studied the saturation behavior of the intensity of the three QDs as a function of the excitation power density per pulse. The results of these measurements are presented in Fig. 2(b).

At low excitation powers ($<5 \text{ W cm}^{-2}$), we observe a linear behavior for all three QDs (with slopes $m_{QD_{bulk}}=0.93$, $m_{QD_{PC1}}=0.88$, and $m_{QD_{PC2}}=1.19$), clearly showing that these lines arise from the radiative recombination of a single electron hole pair (exciton) in the QDs. In strong contrast, at higher excitation power [light gray region in Fig. 2(b)], we observe a clear saturation of the μ -PL intensity as expected for a saturable anharmonic quantum emitter. Saturation corresponds to the situation when each excitation cycle delivers a single photon at the transition energy, meaning that the total photon flux is given by the repetition frequency of the excitation. From these power dependent measurements, we deduce a relative photon extraction enhancement (σ) for QD_{PC1} and QD_{PC2} compared to QD_{bulk} from the ratios of the maximum normalized PL intensities in the saturation regime at 10 W cm^{-2} and obtain $\sigma_{QD_{PC1}}=I_{QD_{PC1}}/I_{QD_{bulk}}=9.9 \pm 1.0$ and $\sigma_{QD_{PC2}}=I_{QD_{PC2}}/I_{QD_{bulk}}=16.4 \pm 1.7$, respectively. This indicates that the light extraction efficiency from a QD in a PC nanostructure without a cavity is already more than ~ 16 times larger than from a QD in bulk GaAs. The difference in the extraction enhancement $\sigma_{QD_{PC1}}$ when compared with $\sigma_{QD_{PC2}}$ arises from a precise local photonic density of states at the position of the QD investigated.¹⁹

The value of σ extracted above represents the *relative* enhancement of the *absolute* photon extraction efficiency η due to the PBG. We now continue to measure the absolute value of η for the investigated QDs by determining the combined photon count rates (Γ^{corr}) on both single-photon counters of a Hanbury Brown–Twiss (HBT) setup for the three QDs investigated. We obtain $\Gamma_{QD_{bulk}}^{corr}=3000 \pm 300$ counts/s for the QD in the bulk material

and $\Gamma_{QD_{PC1}}^{corr} = 20\,000 \pm 2000$ counts/s and $\Gamma_{QD_{PC2}}^{corr} = 40\,000 \pm 4000$ counts/s for the QD_{PC1} and QD_{PC2} , respectively. These measurements were all recorded for excitation powers of 10 W cm^{-2} , where all QDs are close to the saturation regime [c.f. Fig. 2(b)]. Quite generally, η is obtained by dividing the total photon count rate Γ_{QD}^{corr} on both detectors of the HBT by the detection efficiency of the setup $\rho_{detection}$, the quantum efficiency of the detector $\phi_{detector}$ at the detection wavelength,²⁰ and the maximum photon count rate of the QD Γ_{QD}^{max} ,

$$\eta_{QD} = \frac{\Gamma_{QD}^{corr}}{\Gamma_{QD}^{max} \rho_{detection} \phi_{detector}}. \quad (1)$$

In the saturation regime, each excitation pulse results in one, and only one, photon at the exciton transition wavelength. Under these conditions, the maximum photon count rate Γ_{QD}^{max} is determined by the repetition rate of the excitation laser, i.e., $f_{laser} = 80$ MHz. Therefore, we would obtain a maximum photon count rate $\Gamma_{QD}^{max} = 8 \times 10^7$ counts/s emitted from a single QD. In reality, only a small fraction of the emitted photons are detected in our experiment due to emission into guided modes of the GaAs slab, the combined optical losses in the collection system, and finite detector detectivity.

The detection efficiency $\rho_{detection}$ of our measurement setup and its spectral dependence was carefully measured by sending laser light, tuned to the emission wavelength of the three QDs, into the optical detection system. Using a calibrated optical powermeter, we compared the optical power reaching the avalanche photodiode (APD) detector with the optical power entering the collection objective. This procedure resulted in an absolute detection efficiency $\rho_{detection} = 0.875\% \pm 0.1\%$.

By inserting these values in Eq. (1), we obtain $\eta_{QD_{bulk}} = 1.4\% \pm 0.2\%$, $\eta_{QD_{PC1}} = 9.1\% \pm 1.0\%$, and $\eta_{QD_{PC2}} = 24.6\% \pm 2.7\%$ for QD_{bulk} , QD_{PC1} , and QD_{PC2} , respectively.²¹ By comparing these values of η with $\eta_{QD_{bulk}}$, we obtain an enhancement of the extraction efficiencies of 6.5 ± 1.8 times for QD_{PC1} and 17.6 ± 0.9 times for QD_{PC2} , respectively. These values are in excellent agreement with the values presented above for the relative enhancement σ estimated from the power dependent measurements, supporting the validity of our simple analysis.

In Fig. 3(a) (left panel), we present a time-resolved μ -PL spectrum recorded from QD_{bulk} , from which we extract an exciton lifetime $\tau_{bulk} = 0.52 \pm 0.05$ ns, in good accordance with typical values for InGaAs QDs.²² The single-photon character of the QD emission is demonstrated by measuring the second-order correlation function $g^{(2)}(\tau)$ in the saturation regime. For the pulsed Ti:sapphire laser, we obtain a series of equally spaced peaks which correspond to the laser repetition rate (not shown here). However, for a single-photon emitter, the peak at zero delay time should vanish.²³ The measured histogram of QD_{bulk} as a function of the delay time $\tau_1 - \tau_2$ between the two detectors [Fig. 3(a) (right panel)] shows clear signature of photon antibunching from which we determine a reduction of the multiphoton probability to be less than $\sim 19\%$, unambiguously demonstrating the single-photon nature of the emitted light.

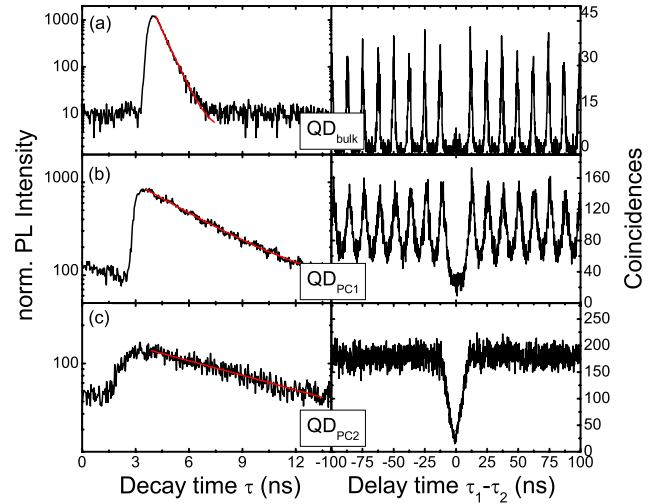


FIG. 3. (Color online) (Left panel) Time-resolved PL data for (a) QD_{bulk} , (b) QD_{PC1} , and (c) QD_{PC2} , respectively. (Right panel) Corresponding photon correlation measurements for (a) QD_{bulk} , (b) QD_{PC1} , and (c) QD_{PC2} , demonstrating clear signature of photon antibunching.

Similarly, we demonstrate the single-photon character of QD_{PC1} and QD_{PC2} inside the PC. QD_{PC1} exhibits a significantly longer lifetime $\tau_{PC1} = 3.7 \pm 0.1$ ns [Fig. 3(b) (left panel)], which originates from the reduced photon density of states inside the PBG.²⁴ Nevertheless, the correlation measurement [Fig. 3(b) (right panel)] indicates strong multiphoton suppression ($\sim 19\%$) evidenced by the absence of the peak at zero delay time. The enhanced background between the adjacent peaks arises due to the larger radiative lifetime of the QD transition, which is reflected in the correlation spectrum by the width of the pulses. This effect is even more pronounced for QD_{PC2} which has a lifetime $\tau_{PC2} = 12.1 \pm 3.0$ ns [Fig. 3(c) (left panel)], comparable to the time between two adjacent laser pulses ($1/f_{laser} = 12.5$ ns). Therefore, peaks are no longer observed in the correlation measurements [Fig. 3(c) (right panel)] but a correlation function that tends toward a constant value away from zero time delay, similar to measurements under continuous wave excitation. The continuous wave like characteristic of QD_{PC2} is also observed in its power dependence [Fig. 2(b), black triangles], which exhibits a decrease of the PL intensity for high pumping powers instead of the saturation expected for pulsed excitation.²⁵ However, the very clear antibunching ($\sim 14\%$) dip close to $\tau_1 - \tau_2 = 0$ ns still confirms the single-photon nature of the emission. The observation of a higher value of η for QD_{PC2} compared with QD_{PC1} combined with the lower SE rate indicates that nonradiative processes can be neglected in our experiment.

The observation of pronounced antibunching in the photon correlation measurements combined with the measurement of the absolute external quantum efficiencies shows that QDs embedded in PC nanostructures are suitable for efficient single-photon generation. The enhanced emission is in very good agreement with systematic time-resolved PL experiments performed on InGaAs QD ensembles in PC nanostructures.¹³ Such an efficient single-photon source is a

promising candidate to be used in quantum cryptography, albeit with a reduced rate for on-demand single-photon generation due to the slowed SE dynamics. When compared to recently demonstrated single-photon generation from QDs in microcavities,^{26,27} our approach is technologically less demanding, since we do not rely on deterministic positioning²⁸ and spectral tuning of emitter²⁹ or mode.³⁰

In summary, we have presented efficient single-photon generation from QDs inside a PBG material. When compared to QDs in bulk GaAs ($\eta_{QD_{bulk}} = 1.4\%$), the incorporation of QDs into a PC nanostructure enhances the external quantum efficiency by a factor close to ~ 16 times and re-

sults in a directly measured absolute extraction efficiency for QDs in the PC of $\eta_{QD_{PC2}} = 25\%$. To the best of our knowledge, this is the highest reported experimental value for the external quantum efficiency in PC nanostructures. Further enhancements would also be possible, for example, by growing a distributed Bragg reflector below the PC slab waveguide in order to suppress radiation into the GaAs substrate.

We acknowledge financial support of the Deutsche Forschungsgemeinschaft via the Sonderforschungsbereich 631, Teilprojekt B3, and the German Excellence Initiative via the “Nanosystems Initiative Munich (NIM).”

*kaniber@wsi.tum.de

- ¹N. Gisin, G. Ribordy, W. Tittel, and Hugo Zbinden, *Rev. Mod. Phys.* **74**, 145 (2002).
- ²E. Knill, R. Laflamme, and G. J. Milburn, *Nature (London)* **409**, 46 (2001).
- ³A. Kuhn, M. Hennrich, and G. Rempe, *Phys. Rev. Lett.* **89**, 067901 (2002).
- ⁴C. Brunel, B. Lounis, P. Tamarat, and M. Orrit, *Phys. Rev. Lett.* **83**, 2722 (1999).
- ⁵B. Lounis and W. E. Moerner, *Nature (London)* **407**, 491 (2000).
- ⁶A. Beveratos, A. Kuhn, R. Brouri, T. Gascoin, J.-P. Poizat, and P. Grangier, *Eur. Phys. J. D* **18**, 191 (2002).
- ⁷C. Santori, M. Pelton, G. Solomon, Y. Dale, and Y. Yamamoto, *Phys. Rev. Lett.* **86**, 1502 (2001).
- ⁸P. Michler, A. Kiraz, C. Becher, W. V. Schoenfeld, P. M. Petroff, L. Zhang, E. Hu, and A. Imamoglu, *Science* **290**, 2282 (2000).
- ⁹M. Pelton, C. Santori, J. Vučkovic, B. Zhang, G. S. Solomon, J. Plant, and Y. Yamamoto, *Phys. Rev. Lett.* **89**, 233602 (2002).
- ¹⁰W.-H. Chang, W.-Y. Chen, H.-S. Chang, T.-P. Hsieh, J.-I. Chyi, and T.-M. Hsu, *Phys. Rev. Lett.* **96**, 117401 (2006).
- ¹¹F. Hofbauer, S. Grimminger, J. Angele, G. Böhm, R. Meyer, M.-C. Amann, and J. J. Finley, *Appl. Phys. Lett.* **91**, 201111 (2007).
- ¹²E. Yablonovitch, *Phys. Rev. Lett.* **58**, 2059 (1987).
- ¹³M. Kaniber, A. Kress, A. Laucht, M. Bichler, R. Meyer, M.-C. Amann, and J. J. Finley, *Appl. Phys. Lett.* **91**, 061106 (2007).
- ¹⁴G. Gilat and L. J. Raubenheimer, *Phys. Rev.* **144**, 390 (1966).
- ¹⁵L. J. Raubenheimer, *Phys. Rev.* **157**, 586 (1967).
- ¹⁶R. Hanbury Brown and R. Q. Twiss, *Nature (London)* **177**, 27 (1956).
- ¹⁷R. Loudon, *The Quantum Theory of Light*, (Clarendon, Oxford, 1983).
- ¹⁸M. Fujita, S. Takahashi, Y. Tanaka, T. Asano, and S. Noda, *Science* **308**, 1296 (2005).
- ¹⁹I. S. Nikolaev, P. Lodahl, A. F. van Driel, A. F. Koenderink, and W. L. Vos, *Phys. Rev. B* **75**, 115302 (2007).
- ²⁰ $\phi_{detector}^{bulk} = 26.3\% \pm 0.6\%$, $\phi_{detector}^{PC1} = 28.2\% \pm 0.6\%$, and $\phi_{detector}^{PC2} = 21.5\% \pm 0.4\%$.
- ²¹The extracted single-photon efficiency was corrected for the multiphoton emission probability by multiplying by $\sqrt{1-g^2(0)}$, where $g^2(0)$ is the amplitude of the autocorrelation response at zero time delay [Fig. 3 (right panel)] (Ref. 9).
- ²²*Single Quantum Dots: Fundamentals, Applications, and New Concepts*, edited by P. Michler (Springer, Berlin, 2003).
- ²³H. J. Kimble, M. Dagenais, and L. Mandel, *Phys. Rev. Lett.* **39**, 691 (1977).
- ²⁴A. Kress, F. Hofbauer, N. Reinelt, M. Kaniber, H. J. Krenner, R. Meyer, G. Böhm, and J. J. Finley, *Phys. Rev. B* **71**, 241304(R) (2005).
- ²⁵J. J. Finley, A. D. Ashmore, A. Lemaître, D. J. Mowbray, M. S. Skolnick, I. E. Itskevich, P. A. Maksym, M. Hopkinson, and T. F. Krauss, *Phys. Rev. B* **63**, 073307 (2001).
- ²⁶K. Hennessy, A. Badolato, M. Winger, D. Gerace, M. Atatüre, S. Gulde, S. Fält, E. L. Hu, and A. Imamoglu, *Nature (London)* **445**, 896 (2007).
- ²⁷D. Press, S. Götzinger, S. Reitzenstein, C. Hofmann, A. Löffler, M. Kamp, A. Forchel, and Y. Yamamoto, *Phys. Rev. Lett.* **98**, 117402 (2007).
- ²⁸A. Badolato, K. Hennessy, M. Atatüre, J. Dreiser, E. Hu, P. M. Petroff, and A. Imamoglu, *Science* **308**, 1158 (2005).
- ²⁹A. Kiraz, P. Michler, C. Becher, G. Gayral, A. Imamoglu, L. Zhang, E. Hu, W. V. Schoenfeld, and P. M. Petroff, *Appl. Phys. Lett.* **78**, 3932 (2001).
- ³⁰S. Strauf, M. T. Rakher, I. Carmeli, K. Hennessy, C. Meier, A. Badolato, M. J. A. DeDood, P. M. Petroff, E. L. Hu, E. G. Gwinn, and D. Bouwmeester, *Appl. Phys. Lett.* **88**, 043116 (2006).